Journal of Geotechnology and Energy | vol. 41 | no. 4 | 2024 | pp. 71–82

https://doi.org/10.7494/jge.2024.41.4.6374

ARTICLE

INVESTIGATION OF SOIL CONDITIONS IN A SELECTED SECTION OF A RAILWAY CUT AS A BASIS FOR DESIGNING GEOENGINEERING WORKS TO IMPROVE THEIR GEOTECHNICAL PARAMETERS

Przemysław Toczek

AGH University of Krakow, Faculty of Drilling, Oil and Gas, Poland
ORCID: 0000-0002-4028-5907
e-mail: toczek@agh.edu.pl

Tomasz Kowalski

AGH University of Krakow, Faculty of Drilling, Oil and Gas, Poland
ORCID: 0000-0002-6767-6342
e-mail: tkowal@agh.edu.pl

Krzysztof Skrzypaszek

AGH University of Krakow, Faculty of Drilling, Oil and Gas, Poland
ORCID: 0000-0003-2358-7361
e-mail: varna@agh.edu.pl

Cezary Cały

PKP PLK S.A, Technology and Laboratory Center in the Silesian Region

Date of submission:
19.06.2024

Date of acceptance:
27.06.2024

Date of publication:
30.12.2024

https://journals.agh.edu.pl/jge

Abstract: One approach to enabling construction, engineering, and mining activities in subsoil with insufficient geo-mechanical properties is to employ innovative methods and technologies. These can effectively modify the physical and mechanical characteristics of the subsoil. The article explores engineering techniques that can enhance the geotechnical properties of soils in locations where they exhibit dysfunctions, such as reduced stability and bearing capacity. Additionally, the paper emphasizes the importance of conducting specific geo-engineering tests to accurately assess the geotechnical conditions. The research directly evaluates the stability of a railway section within the Western Carpathians and presents findings from both field and laboratory tests. Given the instability observed in this section, there is a pressing need for geo-engineering reinforcement measures. These efforts aim to enhance the geotechnical properties and safeguard the railway embankment from potential landslides. Detailed accounts of these remedial works will be the focus of a subsequent study.

Keywords: slopes stabilization methods, geoengineering methods, CPTU probe, rock mass stability analysis, geotechnical tests

1. Introduction

The bearing capacity and stability of subsoil are profoundly influenced by factors such as the degree of consolidation, stress values, and water saturation. To address the challenge of constructing structures in subsoil with subpar geomechanical properties, it's essential to modify the subsoil's physical and mechanical attributes to the desired specifications [1] using innovative techniques.

The design, construction, and subsequent maintenance of engineering structures, transportation infrastructure, hydro-engineering facilities, and the like, invariably present challenges. These challenges necessitate solutions that either enhance the ground's physical and mechanical properties, where necessary, or alter them sufficiently. Such alterations ensure the establishment and sustenance of favorable geo-engineering and geotechnical conditions in susceptible areas.

The issues encountered often stem from intricate geological, hydrogeological, or geomechanical factors, as well as oversights in prior engineering endeavors. A thorough assessment of the geological milieu and the technical constraints specific to the construction site facilitates adjustments to the subsoil's physical and mechanical characteristics beneath engineering structures [1–3].

2. Geoengineering methods

The scope of geoengineering activities feasible in a region is inherently tied to the geological conditions and the physical and mechanical attributes of soils and rocks [1]. These factors significantly influence the design, construction, and utilization of technical infrastructure within the specified area. Figure 1 illustrates the various applications of geoengineering techniques.

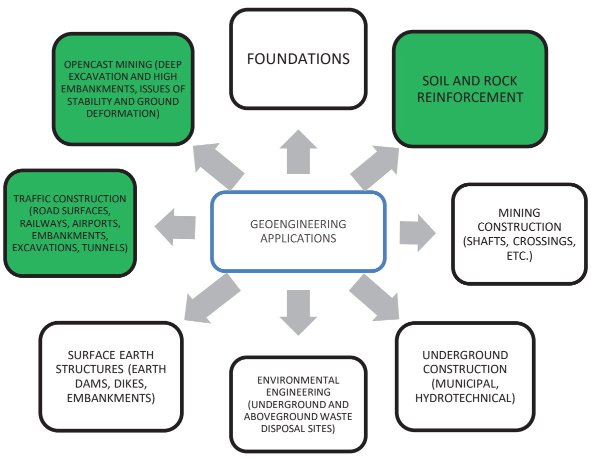

Fig. 1. Own elaboration of geoengineering applications based on [1]

Soil reinforcement plays a crucial role in the construction of various structures, especially when the natural bearing capacity of the soil is insufficient. Approaches to modifying soil properties typically fall into three categories: mechanical, chemical, and physical-chemical methods. Additionally, methods for slope stabilization and protection can be categorized into natural, structural, and synthetic protection, as outlined by Kowacki [4]. Ensuring the stability of slopes, embankments, and excavations remains a paramount concern in the design and execution of civil engineering projects.

Landslides present a significant challenge during the construction, revitalization, and renovation of transport routes. This issue arises not only when attempting to circumvent potential or active landslides but also during the restoration of existing infrastructure facilities [5, 6]. Consequently, accurate forecasting of potential hazards becomes imperative [7]. Addressing the stabilization of escarpments and landslides remains a pressing concern, both in understanding their occurrence and assessing the risks they entail, as well as in advancing scientific methodologies to counteract them [8]. The stabilization of transport-related landslides through structural means has been explored [9], while natural methods and geosynthetics have been discussed [10, 11].

According to the application classification of geoengineering methods, the works were carried out for soil reinforcement to stabilize the landslide along the side of the railway cut surface (Fig. 1 – green color).

Prior to undertaking construction works, it's essential to analyze the existing conditions to determine the most suitable method for modifying the physical and mechanical parameters of the ground. A widely recognized method for such ground investigation is the static CPTU (Cone Penetration Test with Pore Pressure Measurement) sounding [12, 13]. The genesis of this sounding technique can be traced back to the early 1990s [14]. The insights derived from these soundings offer diverse data interpretation avenues, catering to various applications such as landslide investigations [15] or foundational design, including the assessment of pile bearing capacity [13, 16, 17]. Additionally, ground assessment can be enhanced using the SCPTU (static CPTU probe integrated with a seismic module) as discussed by authors [18].

This study offers an analysis conducted using CPTU soundings (Tab. 1) conducted along the railway cut slope (Fig. 2) at designated points Ai, Bi, and Ti. These specific locations were chosen because ground masses exhibited displacement along the slip surface, indicative of the soil medium surpassing its shear strength. The depth and rate of such displacements can vary, resulting in distinct morphological features. The observed landslide formations are attributed to the process of sufosis [19]. This process involves the leaching of soil particles by groundwater in a soil medium characterized by low plasticity, such as silty sands and sandy dust. In the context of this analysis, the formation of these landslides is intrinsically linked to the morphological and geological structures. Their potential occurrence on slopes and inclines is primarily driven by gravitational forces. These formations manifest when the equilibrium between the shear stress components and the soil's resistance is disrupted.

3. Stability analysis as a basis for the design of geoengineering works for slope protection

A comprehensive analysis was conducted to evaluate the stability of the railway cut slopes, particularly in areas where they exhibit instability. To devise an effective solution for ensuring slope stability, it's crucial to pinpoint the factors that contribute to destabilization. A loss of stability typically occurs when shear stresses surpass the shear strength of the soil. Such destabilization can be attributed to various factors, including additional sliding forces, alterations in soil and water conditions, or erosion that diminishes the soil's strength. Often, it's a combination of these factors, making the design of protective measures a multifaceted and intricate process.

In geotechnical endeavors, it is paramount to initially consider the site's morphology and hydrography. A meticulous analysis of the study area lays the groundwork for designing geotechnical interventions, ensuring an accurate assessment of slope stability, embankments, cuts, and other features. Geographically, the area under study is situated in the Western Carpathians. From a geological perspective, it falls within the bounds of the Silesian Plateau, serving as the watershed between the Vistula and Oder river basins. A close examination of the railway line's trajectory on the geological map of Poland, specifically the Cieszyn sheet, reveals that it rests on a bedrock primarily composed of resilient Cretaceous shales interspersed with limestone and thinly-layered marls of the Silesian Mantle. However, certain segments are overlain by Holocene clays, loams, and Pleistocene loess and silts, which offer less-than-ideal support for the railway subgrade's foundation. Despite this fact, an assessment of landslide occurrences sourced from the State Geological Institute's register units (SOPO PIG-PIB 2022) did not indicate any such events in the region under scrutiny. The study commenced with an on-site evaluation, facilitating an in-depth assessment of the geotechnical conditions, encompassing morphology, hydrography, geological structures, and potential site-specific challenges that could influence both design and implementation phases.

In the examined railway cut slopes, a significant issue arises from the presence of a plasticized layer comprised of silty soil. Due to shearing forces, this layer has given rise to a slip plane. The steep gradient of these slopes inherently lacks adequate stabilization, thereby promoting the occurrence of surface soil slides. In alignment with the standards outlined in (PN-EN 1997-1:2008/Ap2, 2010), stability index values were derived from calculated parameters. Notably, these derived parameters were approximately 25% lower than those ascertained through field or laboratory tests, indicating a potential underestimation of the results. The stability analysis was conducted at intervals of 50 m across the evaluated slope section (Fig. 2) in accordance with the following framework:

– Cross-section at km 33+250,
– Cross-section at km 33+300,
– Cross-section at km 33+350,
– Cross-section at km 33+400.

In the article authors were shown cross-section data at km 33+250, km 33+300 and km 33+400 with stability calculations for the slope, both before and after geotechnical works.

In the tables below, the characteristic parameters for mentioned cross-sections are marked (Tabs. 2–4).

Table 1. Depths of CPTU static soundings and boreholes for the case under consideration made from the right – Ai, left – Bi and in the axis of the railway surface Ti of the analyzed slope of the railway cross-section

No.	Measurement point	Probe CPTU [m b.s.l.]	Borehole [m b.s.l.]
1	33+200_T1	4.1	3.5
2	33+200_A	4.1	–
3	33+200_B	6.1	–
4	33+250_T1	4.1	3.5
5	33+250_A	5.2	–
6	33+250_B	7.1	–
7	33+300_T1	4.1	3.5
8	33+300_A	6.6	–
9	33+300_B	6.9	–
10	33+350_T1	4.1	3.5
11	33+350_A	4.8	–
12	33+350_B	6.3	–
13	33+400_T1	4.1	3.5
14	33+400_A	4.1	–
15	33+400_B	4.1	–
16	33+450_T1	3.6	3.5
17	33+450_A	4.1	–
18	33+450_B	4.8	–

During the CPTU examination, various parameters were meticulously recorded at 1 cm depth intervals, including:

- resistance under the probe cone *qc* [MPa]: this parameter was recorded within the range of 0–100 MPa with a resolution of 0.01 MPa,
- friction at the friction sleeve *fs* [kPa]: the values were captured between 0–3000 kPa with a resolution of 0.71 kPa,
- pore pressure at *u*2 [kPa]: this was measured directly behind the cone, beneath the friction sleeve, with values ranging from 0–3000 kPa and a resolution of 0.27 kPa,
- inclination of the cone in both x and y directions [°]: the inclinations were recorded within a ±30° range with a resolution of 0.1°,
- cone penetration velocity *v* [cm/s]: the velocity was gauged with a resolution of 0.08 cm/s.

3.1. Results

The soil type was identified using a Robertson diagram tailored for Polish soils, as specified in (PN-B-04452 2002). To employ this diagram effectively, values for the standardized cone resistance *qt* (accounting for pore pressure *u*2) and the friction coefficient R_f were determined in line with the guidelines (ISO 22476-1 2013). The definitive identification of the soil type is manually executed by the interpreter, who considers data from concurrent investigations, notably geotechnical borings. Parameters reflecting the soil condition were ascertained by following the protocols (PN-B-02480:1998). The compaction degree for non-cohesive soils was deduced using equation:

$$I_D = 0.709 \log q_c - 0.165 \tag{1}$$

The degree of plasticity I_l of cohesive soils (or alternatively the corresponding values of the consistency index I_c), depending on the content of the clay fraction in the layer under consideration *c*:

$$I_l = 0.242 - 0.427 \log q_c, \text{ for } f_i > 30\% \tag{2}$$

$$I_l = 0.518 - 0.653 \log q_c, \text{ for } f_i = 10\text{–}30\% \tag{3}$$

$$I_l = 0.729 - 0.736 \log q_c, \text{ for } f_i < 10\% \tag{4}$$

The assignment of the soils in the investigated soil profile to the appropriate group was made on the basis of a previous interpretation of the soil type and the resulting clay fraction content, according to the classification diagram, the so-called Ferret's triangle (PN-B-02480:1998).

The angle of internal friction φ' of non-cohesive soils was determined based on equation (5) in the standard (DIN 4094:1990-12, 2013), i.e.:

$$\varphi' = 23 + 13.5 \log q_c \tag{5}$$

It is assumed that the above relationship is applicable to non-cohesive soils containing at most a small admixture of fine facies (e.g., silty sands).

For cohesive soils (fine-grained soils) the shear strength under no-drain conditions is determined below:

$$s_u = \frac{q_c - \sigma_{v_0}}{N_k} \tag{6}$$

where are: σ_{v0} represents the vertical total geostatic stress, N_k is an empirical coefficient, the value of which is contingent upon the soil's plasticity index. This index is estimated based on the recommendation from the Swedish Geotechnical Institute, given by the formula $N_k = 13.4 + 6.65 \times w_l$. Here, w_l denotes the liquid limit value, as determined by the table of properties for typical Polish soils, as referenced in [20].

Edometric moduli of soil compressibility for the study area were determined from the standard PN-EN 1997-1:2008, Eurokod 7.

Following the investigations, horizontal layers were identified. The top 1 m below the ground surface consists of silty clays, which also serve as agricultural topsoil. From there, extending to approximately 3.5 m below the surface, brown and grey silty clays exist in a hard plastic state, frequently interspersed with dust layers. This geotechnical assessment pertains to the evaluation of groundwater conditions along railway line no. 190, specifically from km 33+200 to km 33+500, and from km 34+500 to km 34+650 on the Goleszów-Cieszyn route.

In the investigated subsoil, a stratified structure with a horizontal course can be distinguished. In the floor up to a depth of approx. 0.4–1.0 m, there are brown siltstones, which at the same time form an agriculturally cultivated surface. Below, to a depth of approximately 2.5–3.5 m, there is a layer of brown and grey-brown silty clays and hard-plastic silty clays. The above silty clays often contain interbedding of dust. In the bottom of the silty clay, in the section from km 33+250 to km 33+550 (Figs. 3, 5, 7) there is a layer of silty clay of small thickness of approx. 0.5–1.0 m, with a considerable admixture of fine gravel and sand interbeds in plastic and soft plastic state. Below this, grey silty clays with an admixture of gravel were drilled throughout the section, which are generally in a hard-plastic state, with only plastic and soft-plastic in the ceiling. A high concentration of gravel is noticeable in the roof of the above-mentioned silty clays, which is undoubtedly the result of erosional scour and the formation of a "cobble" layer prior to the development of subsequent sedimentary processes.

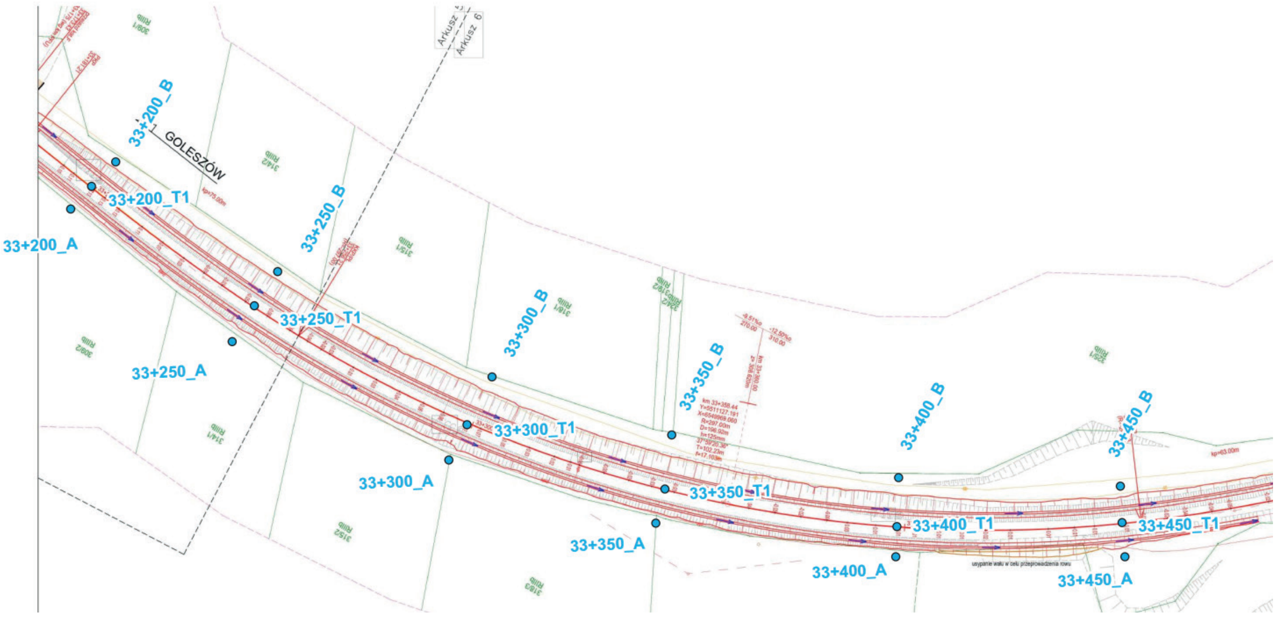

Fig. 2. Characteristic cross-sections across the analyzed slope with an indication of CPTU sounding points

At a depth of approximately 2.5 m from the crown and about 1.5 m from the base of the slope, there is a stratification of degraded, water-softened, soft-plastic dust with a mixture of gravel. This layer is a probable slip plane. The adjacent area to the slope is inclined in its direction. The drainage system directs water to the ditch at the foot of the slope through outlets located at intervals of 30 m at a height of about 1.5 m from the crown of the excavation.

A total of six geotechnical layers were identified within the analyzed cross-section. The layering pattern was established using averaged data from Cone Penetration Test (CPT) with pore pressure measurements (CPTU) and geotechnical boreholes located proximately to the examined cross-section. These geotechnical layers comprised soils of consistent type and origin, displaying analogous values for compaction (in granular soils) or plasticity (in cohesive soils). For these soils, uniform characteristic physical and mechanical parameters were adopted, derived from both CPTU readings and subsequent laboratory tests.

Stability assessments were conducted using design parameters. These parameters were obtained by dividing the characteristic values by a safety factor of 1.25, as raised in standards (PN-EN 1997-1:2008/Ap2:2010, 2010). Mechanical properties (φ', c') of the uppermost slope layers, especially where the outlets of adjacent drainage areas are present, were adjusted using a reduction factor of $\gamma_{red} = 1.4$. Details of the geotechnical layers utilized in the analytical model for selected points are provided in Tables 2–4. It's essential to note that the presented parameters are specific to the examined kilometer of the cross-section and should not be extrapolated universally.

Stability assessments employed the Bishop's method, focusing on a circular slip surface post-optimization, aiming to identify the most plausible path for potential displacements. In the Bishop's method, the interaction forces between the blocks are unknown, and their value is determined by the method of successive trials using general equilibrium equations internal and the stability index is determined from the equilibrium equation of moments of forces relative to the center of the potential slip surface. Figures 4, 6 and 8 illustrates the geological cross-sections with calculations for the designated kilometer at 33+250, 33+300 and 33+400 of the railway line, derived from the comprehensive geotechnical survey.

The presence of these cohesive, plastic soils poses challenges, endangering the stability of slopes and nearby soils along the railway alignment. The inclusion of loose material and sandy layers facilitates water retention across the considered depth, intensifying the plasticization process. Notably, the dust layers are highly vulnerable to plasticization, as even minimal moisture prompts rapid state changes. This vulnerability has led to the formation of a slip edge in this layer (Fig. 5). The geological cross-sections for the designated kilometer at km 33+400 of the railway line, derived from the comprehensive geotechnical survey is shown in Figure 6. Figure 7 presents the cross section with calculations for the mentioned above kilometer point.

Table 2. Characteristic parameters for the selected point 33+250

Geotechnical layer number in 33+400 kilometre range	Type of soil in the layer	Average compaction degree	Degree of plasticity	Reduction coefficient $\varphi'_{red} = \frac{\varphi'}{\gamma_{red}}$ $c'_{red} = \frac{c'}{\gamma_{red}}$	Average parameters		Volume density
	Lithology symbols regarding to PN-EN 1997-1:2008/ Ap2:2010	I_D	I_l	γ_{red}	Angle of internal friction Reduced value	Cohesion Reduced value	
					φ'	c'	ρ
		[–]	[–]	[–]	[°]	[kPa]	[Mg/m³]
Layer I	$G_{\pi z}$	–	0.28–0.37	1.,4	19	8	21
					14	6	
Layer II	$G_{\pi z}$	–	0.14–0.17	1.4	22	12	20.5
					16	9	
Layer III	$G_{\pi z}$	–	0.23–0.25	1.4	17	12	19.5
					12	9	
Layer IV	$G_{\pi z}$	–	−0.18–0.10	1	32	11	22.0
Layer V	$G_{\pi z}$	0.71–0.81	–	1	41	–	20.0
Layer VI	Degraded drainage ditch interior	–	−0.19–0.08	1	10	10	19.0

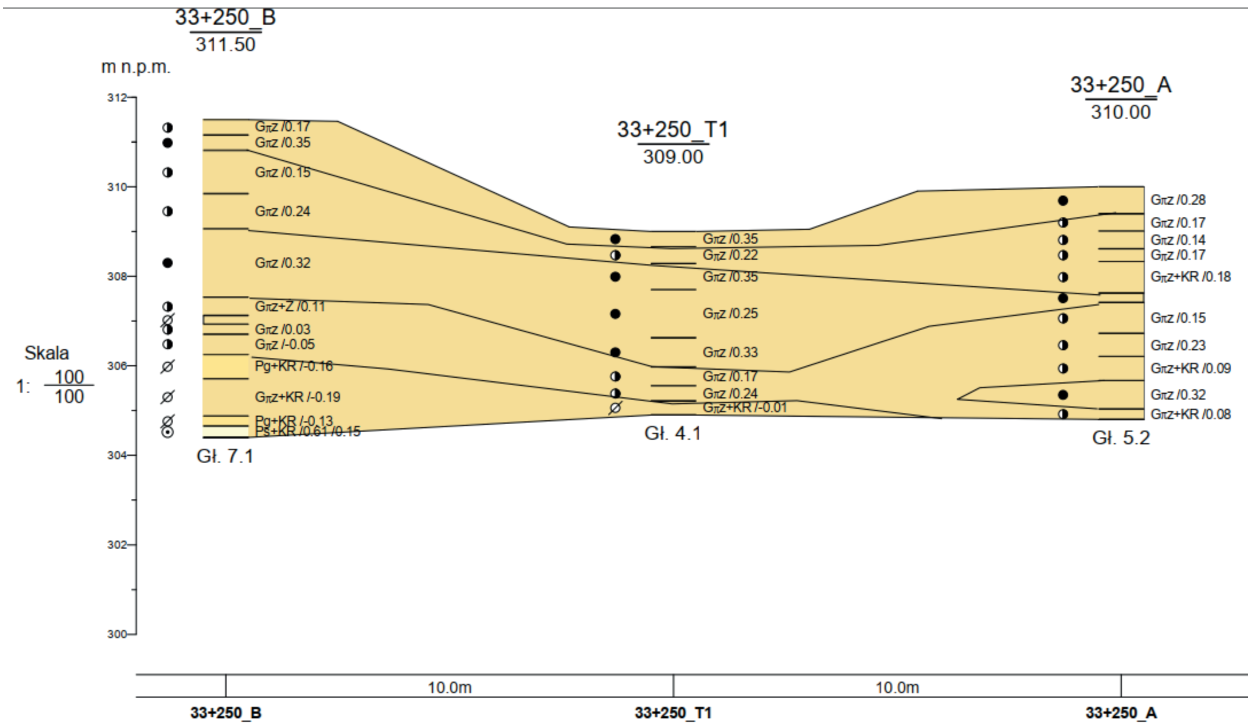

Fig. 3. View of design cross-section with calculations for selected point 33+250 (Geotechnical project BAARS 2020)

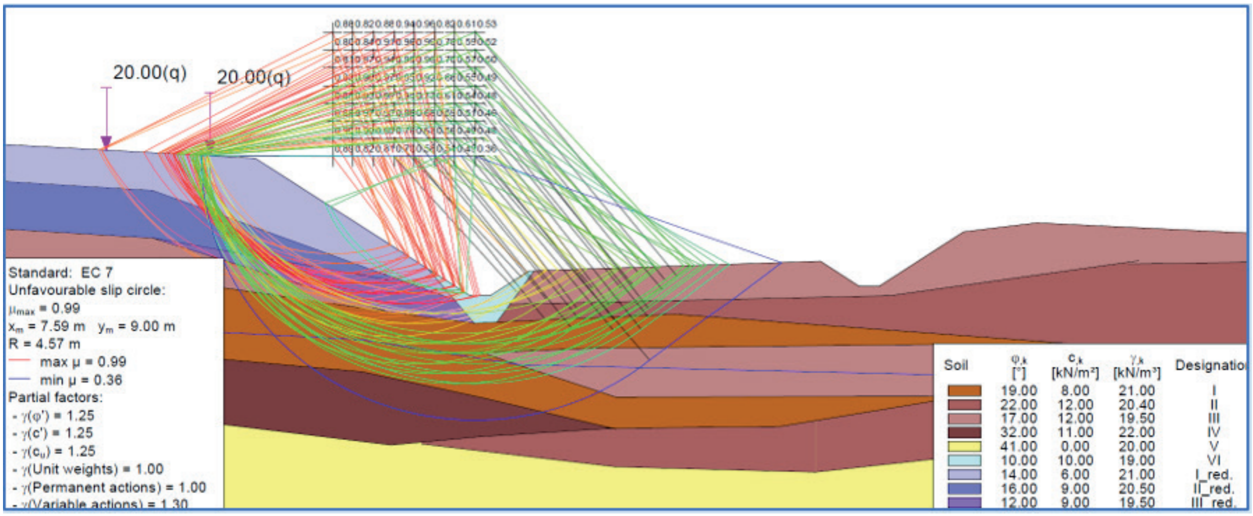

Fig. 4. View of design cross-section with calculations for selected point 33+250 (Geotechnical project BAARS 2020)

Table 3. Characteristic parameters for the selected point 33+300

<table>
<tr><td rowspan="5">Geotechnical layer number in 33+400 kilometre range</td><td>Type of soil in the layer</td><td>Average compaction degree</td><td>Degree of plasticity</td><td>Reduction coefficient $\varphi'_{red} = \frac{\varphi'}{\gamma_{red}}$ $c'_{red} = \frac{c'}{\gamma_{red}}$</td><td colspan="2">Average parameters</td><td rowspan="3">Volume density</td></tr>
<tr><td rowspan="4">Lithology symbols regarding to PN-EN 1997-1:2008/ Ap2:2010</td><td rowspan="3">I_D</td><td rowspan="3">I_l</td><td rowspan="3">γ_{red}</td><td>Angle of internal friction</td><td>Cohesion</td></tr>
<tr><td>Reduced value</td><td>Reduced value</td></tr>
<tr><td>φ′</td><td>c′</td><td>ρ</td></tr>
<tr><td>[–]</td><td>[–]</td><td>[–]</td><td>[°]</td><td>[kPa]</td><td>[Mg/m³]</td></tr>
<tr><td rowspan="2">Layer I</td><td rowspan="2">G_π</td><td rowspan="2">–</td><td rowspan="2">0.15–0.22</td><td rowspan="2">1.4</td><td>20</td><td>10</td><td rowspan="2">21</td></tr>
<tr><td>14</td><td>7</td></tr>
<tr><td rowspan="2">Layer II</td><td rowspan="2">G_π</td><td rowspan="2">–</td><td rowspan="2">0.27–0.31</td><td rowspan="2">1.4</td><td>18</td><td>21</td><td rowspan="2">20.5</td></tr>
<tr><td>13</td><td>15</td></tr>
<tr><td rowspan="2">Layer III</td><td rowspan="2">G_π</td><td rowspan="2">–</td><td rowspan="2">0.50–0.53</td><td rowspan="2">1.4</td><td>13</td><td>12</td><td rowspan="2">19.0</td></tr>
<tr><td>9</td><td>9</td></tr>
<tr><td>Layer IV</td><td>Pg + KR</td><td>–</td><td>–0.02</td><td>1</td><td>27</td><td>7</td><td>22.0</td></tr>
<tr><td>Layer V</td><td>Ps + Ż</td><td>0.90</td><td>–</td><td>1</td><td>40</td><td>–</td><td>20.0</td></tr>
<tr><td>Layer VI</td><td>Degraded drainage ditch interior</td><td>–</td><td>>0.50</td><td>1</td><td>10</td><td>10</td><td>19.0</td></tr>
</table>

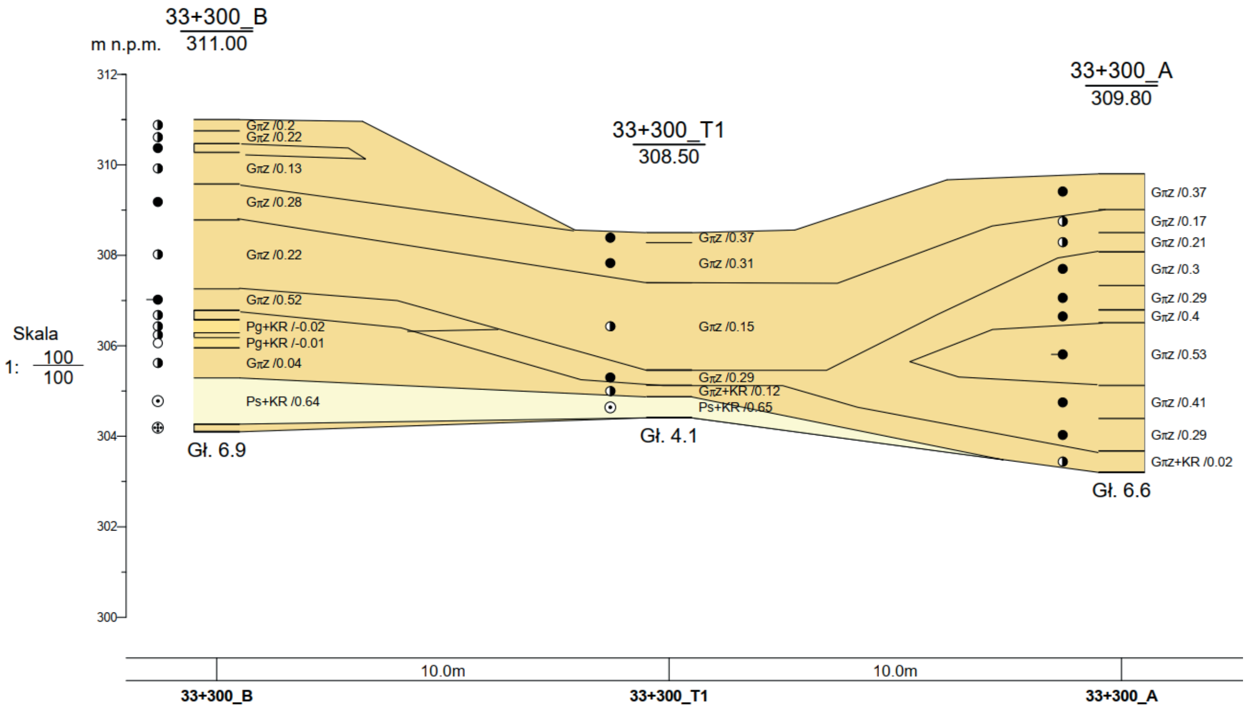

Fig. 5. View of design cross-section with calculations for selected point 33+300 (Geotechnical project BAARS 2020)

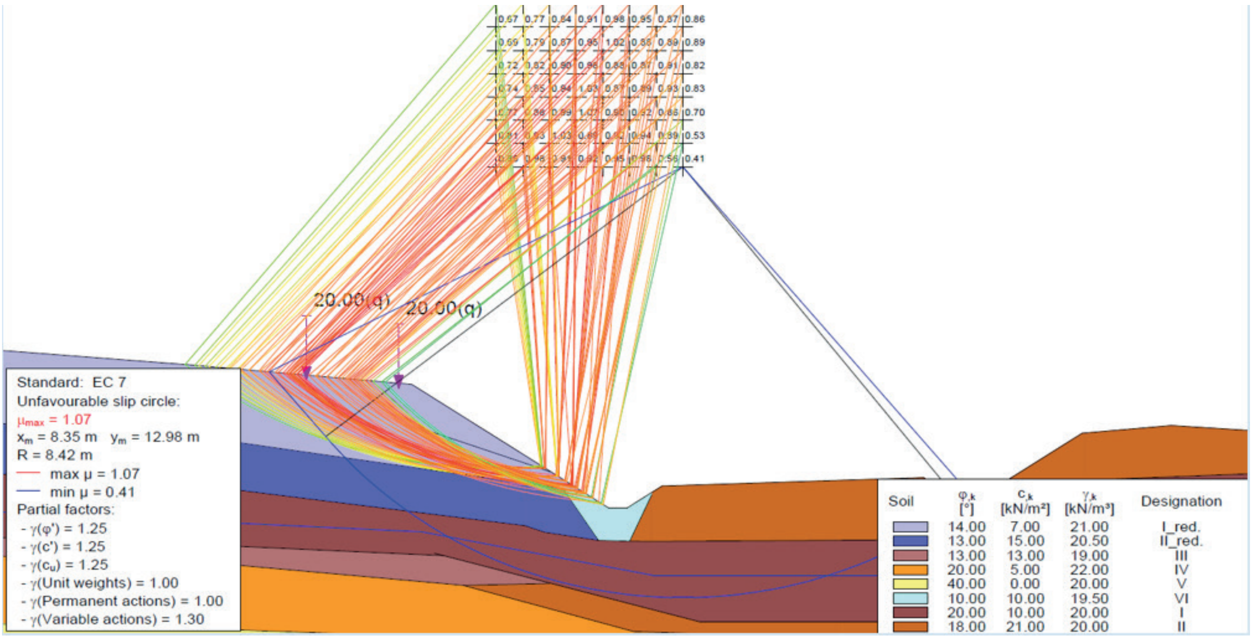

Fig. 6. View of design cross-section with calculations for selected point 33+300 (Geotechnical project BAARS, 2020)

Table 4. Characteristic parameters for the selected point 33+400

Geotechnical layer number in 33+400 kilometre range	Type of soil in the layer	Average compaction degree	Degree of plasticity	Reduction coefficient $\varphi'_{red} = \frac{\varphi'}{\gamma_{red}}$ $c'_{red} = \frac{c'}{\gamma_{red}}$	Average parameters		Volume density
	Lithology symbols regarding to PN-EN 1997-1:2008/Ap2:2010	ID	Il	γ_{red}	Angle of internal friction	Cohesion	
					Reduced value	Reduced value	
					φ'	c'	ρ
		[–]	[–]	[–]	[°]	[kPa]	[Mg/m³]
Layer I	G_{π}	–	0.27	1.4	21	7	20.5
					15	5	
Layer II	$G_{\pi z}/I$	–	0.14	1.4	14	21	21
					10	15	
Layer III	G_{π}	–	0.3–0.37	1.4	14	14	19.5
					10	10	
Layer IV	$G_{\pi z} + KR$	–	0.02–0.11	1	27	12	22.0
Layer V	*KR/KRg*	0.71	–	1	40	–	20.0
Layer VI	Degraded drainage ditch interior	–	>0.50	1	10	10	19.0

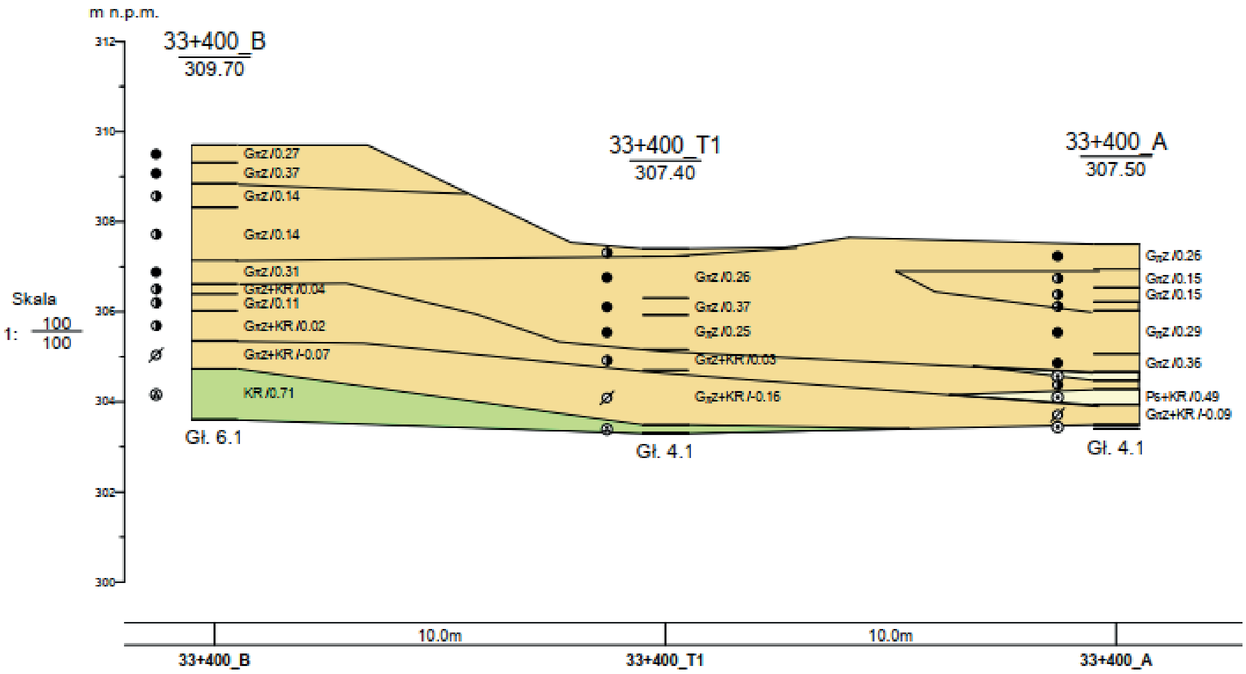

Fig. 7. Geological cross-section for selected point 33+400 (Geological project BAARS, 2020)

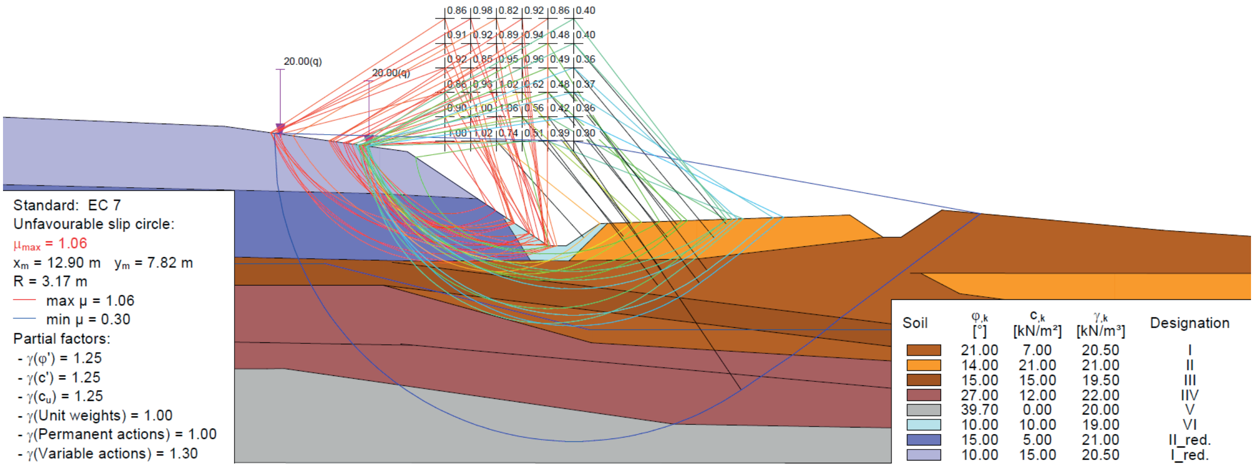

Fig. 8. View of design cross-section with calculations for selected point 33+400 (Geotechnical project BAARS, 2020)

The stability analysis conducted for the railway cut slope at kilometres marker 33+250, 33+300 and 33+400 revealed instability, as indicated by a stability coefficient on the properly Figures 4, 6 and 8.

The stability analysis conducted for the railway cut slope at kilometer marker 33+400 revealed instability, as indicated by a stability coefficient of $F_s = 0.94$. Given the characteristics and results of the stability assessment for the underlying subsoil within this section, it is imperative to undertake design interventions to stabilize the slope at this specific segment of the railway cut.

4. Conclusions

The geotechnical assessment conducted to evaluate the ground conditions of the considered railway line segment highlights significant slope instability. Field and laboratory tests indicate that the instability of the railway cut slope is multifaceted. It arises from a horizontally layered arrangement of strata aligned parallel to the railway cut's direction. This layering encompasses variations in geotechnical parameters, with hard clay layers interspersed with softer, more plasticized zones. The natural subsoil, characterized by its heterogeneity, is highly susceptible to plasticization.

A comprehensive understanding of the soil and hydrological conditions within the examined slope is crucial for designing effective interventions. The primary objective during engineering interventions is to prevent water infiltration into vulnerable layers, particularly at the slip edges and areas of dysfunction.

Within the railway cut's slope, a notable concern is the presence of a plasticized layer of silty soil. This layer has developed a slip plane due to shearing forces. The pronounced slope gradient exacerbates the instability, making the area prone to surface landslides. To mitigate these risks and safeguard against the future threats outlined in the study, it is imperative to develop geotechnical protective measures. These measures should address the potential for mass soil movements along the slip plane within the softer, plasticized dust layers. Various methodologies for such protection will be elaborated upon, drawing parallels to similar challenges encountered in railway cut scenarios.

After all the calculations reinforcement solution were made and it included:

- installing a palisade made of interconnected steel sheet piles anchored with ground spikes to cut through the slip plane,
- reinforcing the slope surface with a concrete anchor and an erosion-resistant geotextile anchored in place,
- strengthening the bottom of the drainage ditch with openwork concrete slabs, filled with dry concrete to prevent soil erosion,
- stabilizing the excavation bottom forming the subgrade with a cementitious binder to prevent the infiltration of rainwater,
- topping the palisade with a concrete anchor and installing linear French drainage behind it,
- directing the drainage to a well at the end of the slope and intermittently to the drainage ditch under the anchor,
- maintaining drainage in the gaps between the sheet piles using a concrete board,
- extending drainage outlets from adjacent agricultural lands at a height of approximately 1.5 m below the slope crown, directing the discharged water to an open ditch at the base of the railway track,
- reinforcing the slope in areas where water is drained from the outlets by installing openwork concrete slabs with voids filled with dry concrete.

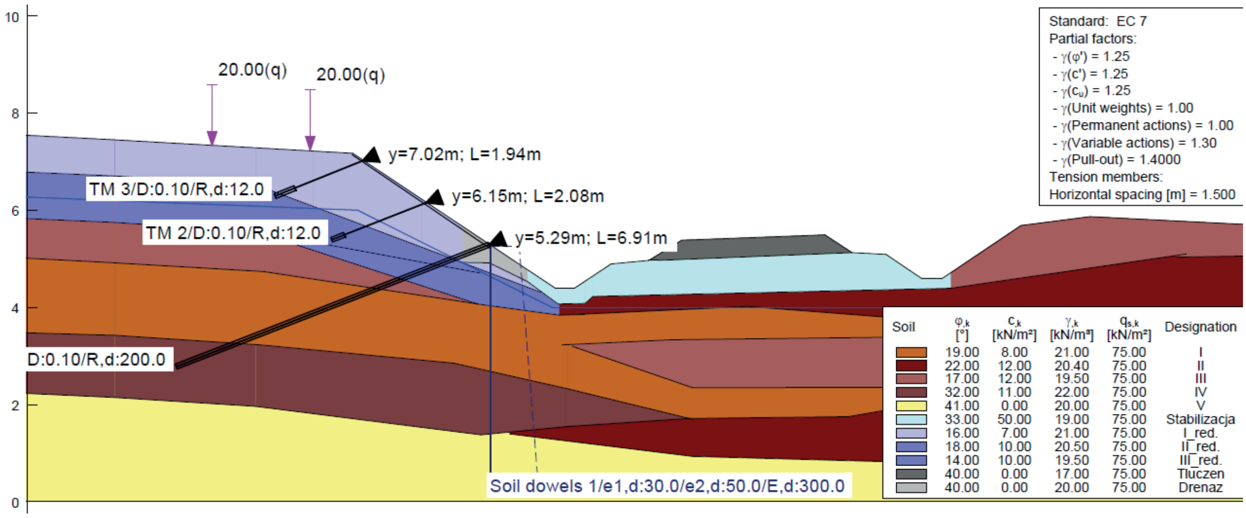

Fig. 9. View of design cross-section with calculations for selected point 33+400 (Geotechnical project BAARS, 2020)

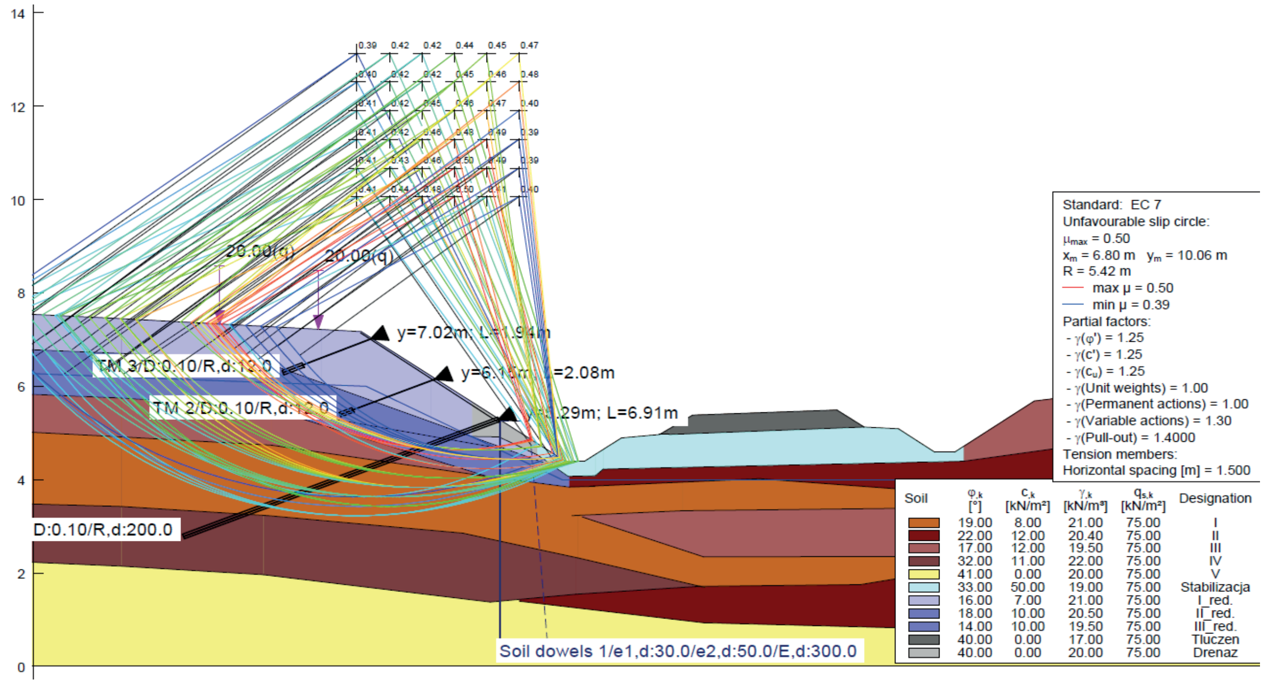

Fig. 10. View of design cross-section with calculations for selected point 33+400 (Geotechnical project BAARS, 2020)

The geotechnical works carried out have improved the stability of slopes within the analyzed section of the railway cutting. In Figures 9 and 10 the cross-section at kilometer 33+250 is shown, along with the applied ground reinforcement and the view of stability calculation results after implementing the proposed solution. The implemented solution has thus achieved a soil stability coefficient above *Fs* = 2.0 for the section at kilometer 33+250, indicating well-executed geotechnical works and slope reinforcement within the analyzed section of the railway cutting.

Author contributions: Conceptualization PT, TK, KS, formal analysis, methodology, writing – review and editing, writing – original draft preparation, and investigation, PT, TK and CC; supervision KS, validation, project administration, PT. All of the authors have read and agreed to the published version of the manuscript

Funding: The project was supported by the AGH University of Krakow, subsidy 16.16.190.779.

Conflicts of Interest: The authors of this paper declare no conflicts of interest.

References

[1] Gonet A., Stryczek S.: *Podstawy geoinżynierii*. Wydawnictwa AGH, Kraków 2020.

[2] Pisarczyk S.: *Geoinżynieria. Metody modyfikacji podłoża gruntowego*. Oficyna Wydawnicza Politechniki Warszawskiej, Warszawa 2005.

[3] Stryczek S.: *Metody geoinżynieryjne modyfikujące właściwości fizyczno-mechaniczne ośrodka gruntowego oraz masywu skalnego*. NTTB Nowoczesne Techniki i Technologie Bezwykopowe, no. 4, Kraków 1999.

[4] Kowacki M.: *Metody stabilizacji i zabezpieczenia terenów osuwiskowych*. Nowoczesne Budownictwo Inżynieryjne, January–February, 2015, pp. 42–47.

[5] Głażewski M., Nowocień E., Piechowicz K.: *Roboty ziemne i rekultywacyjne w budownictwie komunikacyjnym*. Wydawnictwa Komunikacji i Łączności WKŁ, Warszawa 2010.

[6] Kowacki M.: *Stabilizacja skarp i osuwisk*. Nowoczesne Budownictwo Inżynieryjne, May–June, 2019, pp. 88–94.

[7] Wysokiński L.: *Metody prognozowania i zabezpieczania osuwisk (The Methods of Landslides Prediction and Their Protection)*. XXV Konferencja Naukowo-Techniczna „Awarie Budowlane", Międzyzdroje, 24–27.05.2011, pp. 291–320.

[8] Maca N.: *Praktyczne zasady doboru metod stabilizacji osuwisk*. Nowoczesne Budownictwo Inżynieryjne, July–August, 2020, pp. 64–67.

[9] Furtak K., Sala A.: *Stabilizacje osuwisk komunikacyjnych metodami konstrukcyjnymi*. GMDT Geoinżynieria Drogi Mosty Tunele, 3, 2005, pp. 12–22.

[10] Łęcki P., Różański M.: *Wzmacnianie podłoża gruntowego budowli drogowych*. Nowoczesne Budownictwo Inżynieryjne, March–April, 2015, pp. 46–54.

[11] Bzówka J.: *Wybrane techniki wzmacniania słabego podłoża gruntowego w budownictwie komunikacyjnym*. Inżynieria Morska i Geotechnika, 3, 2015, pp. 416–423.

[12] Bagińska I.: *Analiza oceny rodzaju gruntu ustalonego na podstawie badań CPTU (An analysis of the assessment of the type of soil based on the CPTU study)*. Geoinżynieria: Drogi, Mosty, Tunele, 37, 2, 2012, pp. 38–45.

[13] Czado B., Pietras J.S.: *Comparison of the cone penetration resistance obtained in static and dynamic field tests*. AGH Journal of Mining and Geoengineering, 36, 1, 2012, pp. 97–105.

[14] *Engineering Geology Field Manual: Volume II, Chapter 22*, U.S. Department of the Interior Bureau of Reclamation, 2001.

[15] Bednarczyk Z.: *Landslide Investigations by Static Sounding with Pore Pressure Measurements (CPTU), Ground Penetration Radar Techniques (GPR) and Other Chosen Methods*. Conference "Risks Caused by the Geodynamic Phenomena in Europe", Polish Geological Institute Special Papers, 15, 2004, pp. 19–28.

[16] Bagińska I., Sacha M.: *Przygotowanie wyników sondowania statycznego CPTU a proces projektowania nośności pala wciskanego (Preparation of the results of static CPTU probing and the process of designing the load-bearing properties of driven piles)*. GDMT Geoinżynieria Drogi Mosty Tunele, 56, 3, 2016, pp. 14–18.

[17] Eslami A., Moshfeghi S., Mola Abasi H., Eslami M.: *Piezocone and Cone Penetration Test (CPT and CPT), Applications in Foundation Engineering*. Elsevier, Butterworth-Heinemann, 2019.

[18] Jędrysiak N., Bagińska I.: *Rozpoznanie podłoża gruntowego sondą SPCTU (The identification of subsoil with an SCPTU probe)*. Górnictwo i Geoinżynieria, 34, 2, 2010, pp. 341–349.

[19] Stryczek S., Gonet A., Wiśniowski R.: *Geoinżynieryjne metody stabilizacji skarp i zboczy*. Nowoczesne Budownictwo Inżynieryjne, 6, 2008, pp. 78–81.

[20] Wiłun Z.: *Zarys geotechniki*. Wydawnictwa Komunikacji i Łączności WKŁ, Warszawa 2013.